Time-resolved rheology as a tool to monitor the progress of polymer degradation in the melt state – Part I: Thermal and thermo-oxidative degradation of polyamide 11

G. Filippone [a, *], S.C. Carroccio [b, *], R. Mendichi [c], L. Gioiella [a], N.Tz Dintcheva [d], C. Gambarotti [e]

[a] *Dipartimento di Ingegneria Chimica, dei Materiali e della Produzione Industriale (INSTM Consortium - UdR Naples), Università di Napoli Federico II, Piazzale V. Tecchio 80, 80125 Napoli, Italy*

[b] *Consiglio Nazionale delle Ricerche, CNR-IPCB UOS Catania, Via P. Gaifami 18, 95126 Catania, Italy*

[c] *Istituto per lo Studio delle Macromolecole (ISMAC) Consiglio Nazionale delle Ricerche (CNR), Via E. Bassini 15, 20133 Milano, Italy*

[d] *Dipartimento di Ingegneria Civile, Ambientale, Aerospaziale, dei Materiali, Università di Palermo, Viale delle Scienze, Ed. 6, 90128 Palermo, Italy*

[e] *Dipartimento di Chimica, Materiali e Ingegneria Chimica "Giulio Natta", Politecnico di Milano, Piazza L. da Vinci 32, 20133 Milano, Italy*

Received 3 May 2015
Accepted 30 June 2015
Available online 14 July 2015

1. Introduction

Rheology is very sensitive to changes in the molecular architecture of polymeric materials. Any change in the molecular architecture, e.g. chain extension/scission, branching, cross-linking, affects the mobility of the entire chain or of a fraction of it, with immediate, clear repercussions on the polymer relaxation spectrum. This makes rheology a useful tool for studying degradation phenomena in the melt state. Compared to common steady-shear rheology, linear viscoelastic analysis (LVA) is preferable for this purpose, as it involves small amplitude oscillations that do not alter the evolving molecular structure while testing. In principle, a simple frequency scan can provide information on the polymer dynamics over different length scales, from few repeating units up to the sizes of the entire chain. Studying the latter, however, may be challenging. The reason is that the larger is structural unit to be probed, the longer is its characteristic relaxation time, and, hence, the lower is the mechanical frequency to be used. On the other hand, low frequency means long experimental times. More precisely, the minimum time required to collect viscoelastic data at a frequency ω is $t_{ext} = 2\pi/\omega$. In other words, the duration of common LVA measurements can exceed the characteristic time of the degradation phenomenon to be studied. This is one of the reasons which prevented a systematic employ of rheological techniques for monitoring and studying degradation of polymer melts. Speeding

* Corresponding authors.
E-*mail addresses:* gfilippo@unina.it (G. Filippone), sabrinacarola.carroccio@cnr.it (S.C. Carroccio).

the analyses without renouncing to probe low frequencies is hence crucial. To conciliate these two opposite requirements, we resort to time-resolved mechanical spectroscopy (TRMS) [1]. TRMS essentially consists in studying the viscoelastic properties as a function of time rather than in terms of the mechanical frequency. As such, TRMS allows determining frequency-dependent data and relaxation time spectra at intermediate states of transient materials. Many polymer systems belong to this category, e.g. polymer blends [2–4], gels [5,6], thermosets [7–9], nanocomposites [10]. Here we discuss the benefits of TRMS in the study of polymer degradation in the melt state. Besides the scientific interest, this matter is also relevant from a technological point of view. Indeed, the overwhelming majority of the transforming technologies of polymeric materials entails melt processing steps that can alter the polymer structure and, through it, the final material performances. Moreover, changes in the molecular architecture have a direct impact on the material processability, possibly inducing flow instability phenomena [11–13].

The polymer selected for this study is nylon 11 (PA11). It is a bio-based polyamide often used in flexible pipe applications for offshore oilfield exploration or, blended with polyolefins, for diesel and gasoline fuel tanks. Degradation of polyamides is a complex process that has been the subject of many studies, which differ among them for the analytical techniques employed and the conditions in which degradation has been investigated [14–21]. In this regard, it is worth noting that the literature on polyamide degradation in the molten state is pretty scarce [22–24]. Referring to specific papers for the chemical aspects, here we simply observe that PA11 degradation in the melt state can lead to chain scission, chain extension and/or cross-linking, and that these reactions can occur singly or in combination depending on the amount of water and the presence of oxygen. This makes PA11 a challenging testbed for our study, which consists in a critical discussion about the po-tentiality of rheological analysis for the study of polymer degradation in the melt. The work is divided in two distinct papers. In *Part I* we deal with pure PA11, which has been subjected to rheological measurements in both N_2 and air environment aiming at studying the effects of thermal and thermo-oxidative degradation. In more detail, the first part of the paper is devoted to prove the advantages of TRMS techniques when the goal is studying fast degradation phenomena. Accurate viscoelastic data are collected and correlated to the changes in the molecular architecture. The conclusions drawn on the basis of rheological analysis are supported by means of size exclusion chromatography (SEC), while matrix-assisted laser desorption/ionization time-of-flight (MALDI-TOF) mass spectrometry is employed to shed light on the structural changes due to degradation. Like any other analytical techniques based on the analysis of polymer solutions, SEC and MALDI-TOF cannot provide direct information about cross-linking reactions, which results in insoluble gel fractions. On the contrary, we show that rheology promptly detects even small amounts of cross-linked polymer. Overall, our analysis provides useful guidelines for a profitable use of rheological techniques in the field of degradation of polymeric materials in the melt state. The study continues in *Part II*, where the implications stemming from the presence of nanoparticles, which are able to remarkably alter the rheology of the host polymer, are critically discussed [25].

2. Experimental

2.1. Materials and sample preparation

The PA11 (Sigma–Aldrich) has $\rho = 1.026$ g cm^{-3} at $T = 25$ °C, glass transition temperature $T_g = 46$ °C and melting temperature $T_m = 198$ °C. 2-(4 hydroxyphenilazo)benzoic acid (HABA) and hexafluoroisopropanol (HFIP) were purchased from Aldrich Chemical CO (Italy) and used as supplied.

Rheological tests were performed directly on the pellets of PA11. The samples for the SEC and MALDI analyses were prepared by treating the polymer under either nitrogen or air atmosphere at $T =$ 215 °C for 30, 60, 90, 120 and 150 min. Then the materials were dissolved in HFIP, and the solutions were filtered and dried before analyses. Fractions of insoluble gel, if any, were dried under vacuum and weighed.

2.2. Characterization

2.2.1. Rheological tests

Rheological analyses were carried out using a stress-controlled rotational rheometer (AR-G2 by TA Instruments) in parallel plate geometry (plate diameter 40 mm). The pellets of PA11 were compacted between the plates by means of a containment ring, which was removed before running the tests. The measurements were carried out after drying the polymer for 18 h at $T = 80$ °C under vacuum. Frequency scans were performed at $T = 215$ °C from frequency $\omega = 10^{-1}$ up to 10^2 rad s^{-1}. This range represents a compromise to meet two opposite requirements: (*i*) the need to investigate timescales long enough to provide information on the behavior of large portions of the polymer chains, and (*ii*) the necessity of containing as much as possible the experimental times so to accurately detect degradation phenomena. The latter were monitored during time by means of repeated frequency scans. The elastic (G') and viscous (G'') shear moduli were recorded at strain amplitude low enough to be in the linear regime, which was preliminarily estimated for each sample through strain scan experiments.

2.2.2. Molecular characterization by a SEC-MALS chromatographic system

The molar mass distribution (MMD) of polymers was determined by a multi-detector size exclusion chromatography (SEC) system using two on-line detectors: (*i*) a multi-angle light scattering (MALS); (*ii*) a differential refractometer (DRI) as concentration detector. The SEC-MALS system consists of an Alliance 2695 separation module from Waters with a serial setup Alliance-MALS-DRI. Experiments were carried out at $T = 40$ °C using two PLgel Mixed C columns (5 μm particle size) from Polymer Laboratories. Hexafluoro-2-Propanol (HFIP) + 0.02 M Tetraethylammonium Nitrate salt was used as mobile phase. The flow rate was 0.5 mL/min of flow rate, and the sample concentration was ~3 mg/mL.

The MALS on-line detector uses a vertically polarized He–Ne laser (wavelength 632.8 nm) and measures simultaneously the intensity of the scattered light at 18 fixed angular locations ranging 14.0°–166.0°. An on-line MALS detector coupled to a concentration detector allows to obtain the absolute molar mass and the radius of gyration of each fraction of eluting polymer. The calibration constant was calculated using toluene as standard, assuming a Rayleigh factor of 1.406×10^{-5} cm^{-1}. The angular normalization of the different photodiodes was performed by measuring the scattering intensity of a poly(methyl methacrylate) standard. The use of a multi-detector SEC-MALS system was described in more detail in the literature [26,27].

2.2.3. MALDI-TOF analysis

MALDI-TOF mass spectra were recorded in reflector mode using a Voyager-DE STR (Applied Biosystems) mass spectrometer equipped with a nitrogen laser emitting at 337 nm with a 3-ns pulse width and working in positive ion mode. The accelerating voltage was 20 kV; the grid voltage and the delay time were optimized for each sample to achieve the higher molar mass values and the best

resolution. The laser irradiance was maintained slightly above threshold. 2-(4-hydroxyphenilazo) benzoic acid (0.1 M in HFIP) was used as matrix. Appropriate volumes of polymer solution (5 mg/mL in HFIP) and matrix solution were mixed to obtain 2:1, 1:1, and 1:2 ratios (sample/matrix v/v). 1 μL of each sample/matrix mixture was spotted on the MALDI sample holder and slowly dried to allow matrix crystallization. At least three separate PA11 portion were analyzed at each heating time. The resolution of the reported MALDI spectra is about 9000–12,000 full-width half-maximum, and the accuracy of mass determination was about 160 ppm in the mass range 1000–2000 Da, and 230 ppm in the mass range 2000–3000 Da. The structural identification of MALDI peaks was mainly based on empirical formulas. However, isotopic resolution considerably helped in the peak-assignment process through the comparison of the relative intensities of isotopic peaks corresponding to oligomers of increasing molar mass [20].

3. Results

3.1. TRMS - thermal and thermo-oxidative degradation

The high sensitivity of the flow behavior of polymeric materials to their molecular architecture suggests the employ of rheology to study degradation phenomena. On the other hand, the changes can be so rapid to alter the outcomes of rheological tests. As a result, getting the mere relaxation spectrum of the material can be challenging. As an example, the viscoelastic moduli of PA11 estimated through two consecutive frequency sweep experiments are shown in Fig. 1. The tests were carried out in dry N_2 from low to high frequency.

The comparison between first and second scan shows that the moduli increase while testing. More precisely, the growth is so fast that alterations occur even in the course of the single frequency scan. This can be inferred by looking at the power-law dependences of the moduli at low frequency, which exceed the limiting behavior $G' \sim \omega^2$ and $G'' \sim \omega^1$ predicted in case of terminal Maxwellian behavior. The reason is an overestimate of the moduli as the test proceeds from low to high frequencies. In addition, it should be observed that the time interval between consecutive data captures shortens with increasing the frequency (see inset of Fig. 1). This further contributes in distorting the relaxation spectrum.

To sum up, conventional viscoelastic analysis by means of frequency scans is not suited for a thorough study of materials like PA11, which experience fast degradation phenomena. To overcome these problems and get the mere frequency dependence of the viscoelastic moduli, we use TRMS. In particular, a simple testing procedure based on a time sequence of frequency scans was defined. Provided the duration of each scan is short enough, an accurate estimate of the time evolution of the viscoelastic moduli can be obtained by plotting the moduli as a function of the acquisition time. This is shown in Fig. 2, where the elastic moduli of PA11 collected in N_2 and in air by means of 28 consecutive frequency scans are reported. The viscous moduli exhibit similar but weaker time-dependence (see Figure S1, Supplementary data).

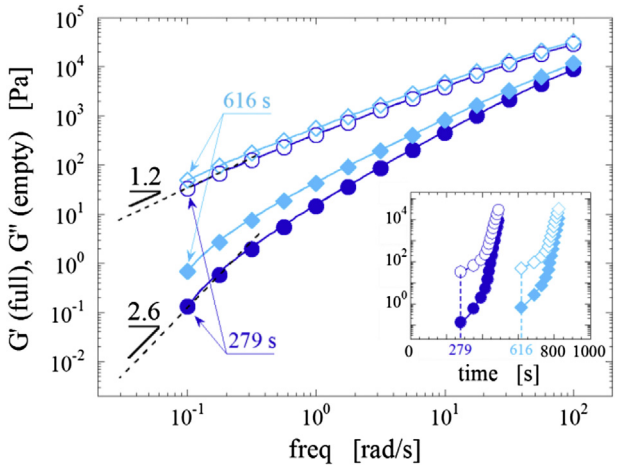

Fig. 1. Linear viscoelastic moduli of pure PA11 in N_2 collected during two consecutive frequency scans (circles: first scan; diamonds: second scan). The same data are shown in the inset as a function of the acquisition time.

At each frequency ω the modulus increases with a certain time-dependence, which reflects the degradation of the specific dynamic population that relaxes in a characteristic time $\tau = 2\pi/\omega$. The high-frequency behavior returns the effect of degradation on the dynamics of small fractions of polymer chain, which alone are able to adapt to rapid deformations. It is not surprising that this population is only slightly affected by degradation. Much more important is the effect at low frequency, where the response of large portions of chain is probed. In this regime, degradation-induced alterations in the molecular architecture have a remarkable effect on the overall elasticity, which rapidly grows of several orders of magnitude.

Our first purpose was inferring the behavior of the polymer before the occurrence of any degradation effect. The quite regular trend of the curves of Fig. 2 allows for a reliable estimate of the moduli at time-zero, i.e. of "virgin" PA11. This extrapolation procedure is described in detail in the Supplementary data (see Figure S2); the so obtained moduli of PA11 at time-zero are shown in Fig. 3.

The accuracy of the extrapolation procedure is proved by the perfect overlap of the curves extrapolated from measurements carried out in N_2 and in air: the behavior of "virgin" PA11 cannot depend on the environment. The moduli scale with frequency as $G' \sim \omega^2$ and $G'' \sim \omega^1$, which means that virgin polymer is fully relaxed in the course of the whole test. More precisely, its terminal relaxation time is $\tau_0 = 2\pi \times \lim_{\omega \to 0} \frac{G'}{\omega G''} \approx 0.04$ s [28], that is shorter than the characteristic time of the oscillation at the highest investigated frequency, $\tau_{min} = 2\pi/\omega_{max} = 0.063$ s. It is worth noting the remarkable overestimate of the moduli collected by means of a simple frequency scan performed soon after having loaded the sample between the plates of the rheometer (gray diamonds in Fig. 3). Quantitative disagreement apart, we stress once again that the shape of the curves is noticeably distorted because of the degradation phenomena which occur while testing.

Before discussing the time evolution of the rheological properties due to degradation, the results of SEC and MALDI-TOF analyses are briefly summarized to provide additional information about the structure of pristine PA11. The average molar mass and polydispersity index of virgin PA11 resulted from SEC are $M_w = 28.8$ kDa and $M_w/M_n = 1.72$, respectively. MALDI-TOF reveals that the original PA11 sample is essentially constituted by linear chains terminated with carbonyl groups at one hand and amino groups at the other extremity of the chain ($COOH/NH_2$). Cyclic oligomers were also noticed at lower mass range region (see Figure S3, Supplementary data).

3.2. Time evolution of the rheological properties

Once the initial properties of the polymer have been established, we can focus on the kinetics of the degradation phenomena. Now the goal is collecting the moduli as a function of time, so as to monitor the progress of degradation from its effect on the rheological properties. Rather than referring to the outcomes of single frequency scans, which suffer from changes in the viscoelastic properties in the course of the test, we consider the "isochronal"

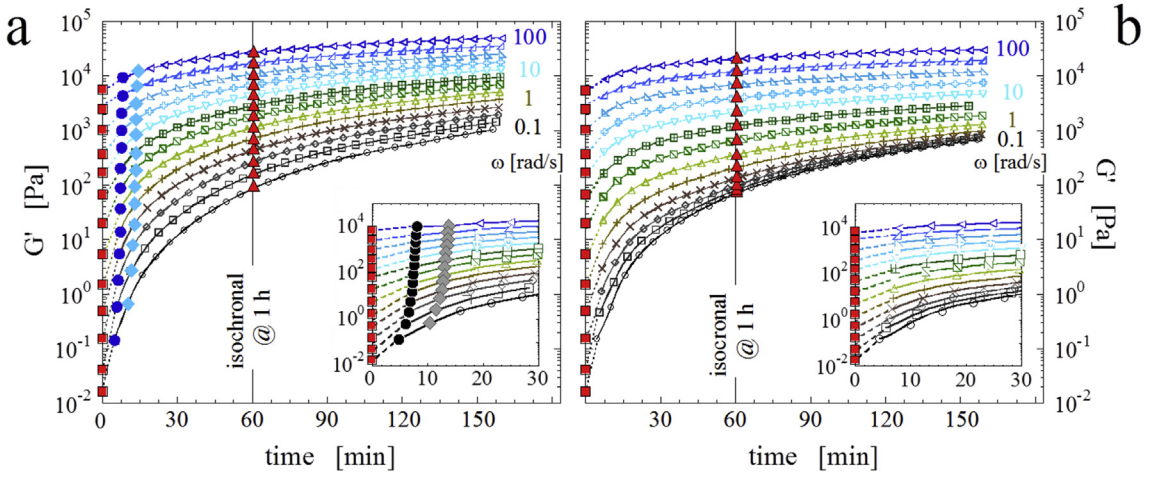

Fig. 2. Time evolution of the elastic moduli of PA11 at $T = 215\,^{\circ}C$ in N_2 (a) and in air (b). Red squares and triangles represent the extrapolated moduli at time-zero and the isochronal moduli at 60 min, respectively. Circles and diamonds in the plot on the left hand side are the elastic moduli of the first and second frequency scan already shown in Fig. 1. The insets show magnifications of the plots in the first 30 min. (For interpretation of the references to colour in this figure legend, the reader is referred to the web version of this article.)

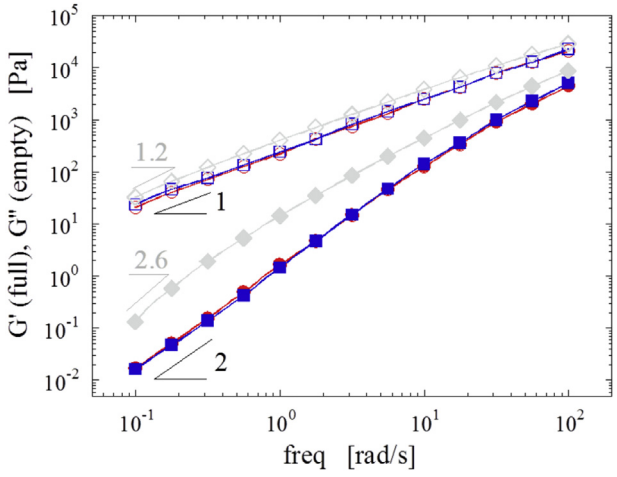

Fig. 3. Moduli of PA11 extrapolated at time-zero from tests carried out in N_2 (blue squares) and in air (red circles). Gray diamonds are the moduli collected through a simple frequency scan performed soon after having loaded the sample between the plates of the rheometer (shown as blue circles in Fig. 1). (For interpretation of the references to colour in this figure legend, the reader is referred to the web version of this article.)

moduli, easily obtainable at any instant t^* as the intercepts between a vertical line at t^* and the curves that interpolate the experimental points (see Fig. 2) [29]. Such accurate snapshots of the viscoelastic behavior are shown in Fig. 4 at different instants.

Quantitative and qualitative differences emerge between the two samples since the early stages of the tests. In particular, the moduli of the sample tested in N_2 are generally higher than those treated in air. Moreover, a peculiar low-frequency plateau of G' is noticed in the latter sample. Such an arrest of relaxation dynamics indicates long-range connectivity, which involves increasing fraction of polymer chains over time. By contrast, only a gradual slowdown of the relaxation dynamics is noticed in N_2.

A simple qualitative analysis of Fig. 4 allows to venture some guesses about the degradation mechanisms. The gradual evolution of the viscoelastic response of PA11 in N_2 is consistent with a progressive increase of the molecular weight of the polymer. More precisely, we argue that post-condensation reactions could the dominant mechanism in a dry N_2 atmosphere, where the amount of water, probably lower than what prescribed by thermodynamic equilibrium, drives the system towards further polymerization. In contrast, the clear arrest of relaxation processes noticed in air suggests more radical alterations in the molecular architecture. In particular, cross-linking reactions could explain the rheological response over long times. However, the occurrence of concurrent degradation reactions cannot be excluded. In particular, oxygen and air moisture could promote chain scission and hydrolysis reactions [23,30,31]. In the next Section we discuss how to discriminate among these possible degradation mechanisms by means of rheological analysis.

3.3. Correlations between rheological data and polymer degradation

The high accuracy of the rheological curves collected by means of TRMS allows for a rigorous analysis of the alterations in the polymer relaxation spectra due to degradation. In this regard, the complex viscosity curves $\eta^*(\omega)$, are particularly rich of information. The latter, computed using the isochronal moduli of Fig. 4, are shown in Fig. 5 at different instants.

At time-zero the behavior is essentially Newtonian, which is a direct consequence of the relaxed state of virgin PA11 in the whole range of investigates frequencies. Afterwards the behaviors differentiate in the two gases, reflecting the changes in the relaxation spectra discussed before: the slowdown of the relaxation dynamics in N_2 results in the narrowing of plateau of η^* at low frequency; in the same range, the upturn of the viscosity curves in air reveals the arrest of the relaxation processes.

To study in detail the time evolution of the rheological properties, the following model was fitted to the experimental data:

$$|\eta^*(\omega)| = \frac{\eta_0^*}{[1+\lambda\omega]^{1-n}} + \frac{\sigma_0}{\omega} \qquad (1)$$

Equation (1) is a simple Carreau-like equation corrected by a yield stress that accounts for the arrest of relaxation dynamics of the samples treated in air. The rationale for using Equation (1) originates from the precise physical meaning of its parameters, which determine the shape of the $\eta^*(\omega)$ curves as outlined in Fig. 6. In particular: η_0^* is the zero−frequency complex viscosity; λ represents the main relaxation time of the polymer; n, usually referred as "flow index", quantifies the non-Newtonian feature of

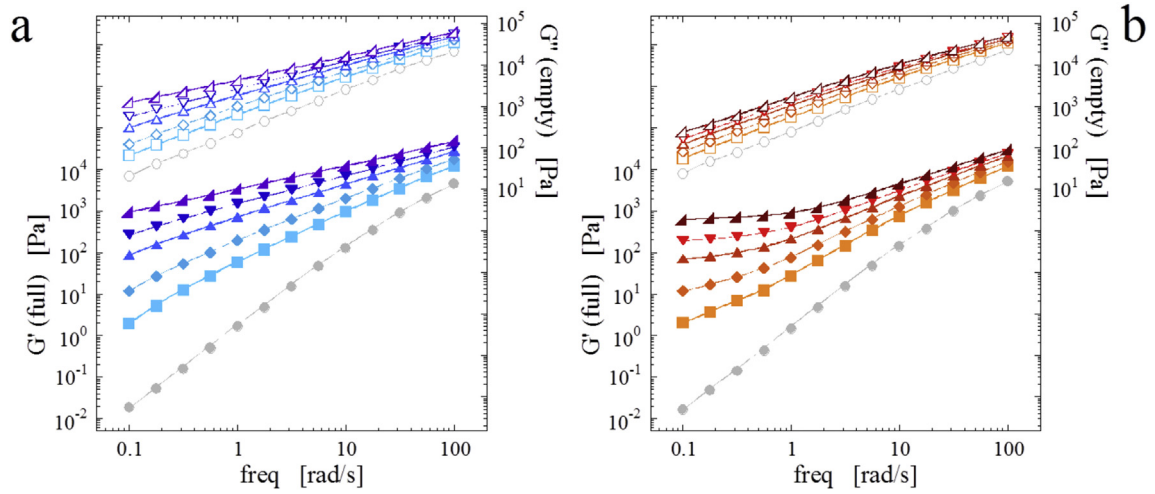

Fig. 4. Isochronal elastic (full symbols, left axis) and viscous (empty symbols, right axis) moduli of PA11 treated in N_2 (a) and in air (b) at different instants: from bottom to top, 15, 30, 60, 90 and 150 min. The circles are the moduli at time-zero (the same as in Fig. 3).

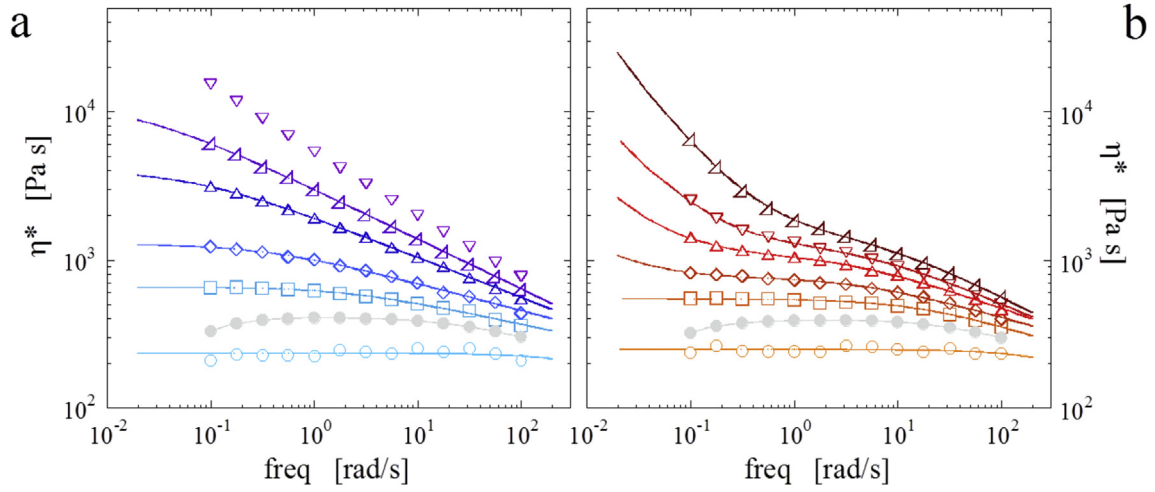

Fig. 5. Isochronal complex viscosity of PA11 treated in N_2 (a) and in air (b) at different instants from bottom to top (empty symbols) 0, 15, 30, 60, 90 and 150 min. The continuous lines are the fitting of Equation (1) to the experimental data. Gray full circles are the outcome of simple frequency scans performed soon after sample loading.

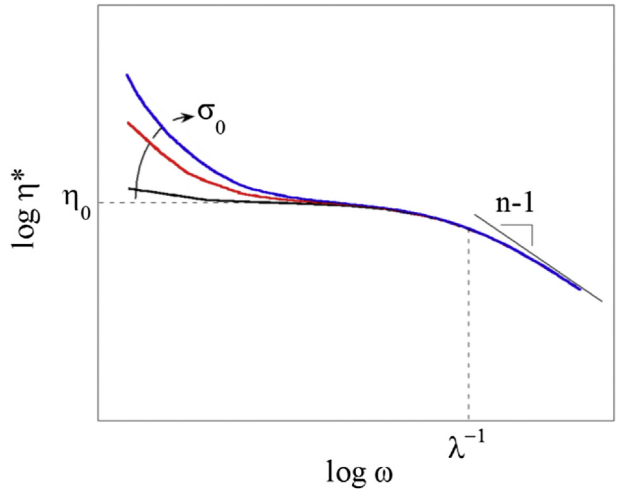

Fig. 6. Graphical description of the parameters of Equation (1).

the polymer; σ_0 is the maximum shear stress that the polymer can sustain before starting to flow. As such, it differs from zero only in case of some internal structure that confers solid-like features to the polymer. In this case, an upturn of η^* is noticed at low frequency. As far as our samples are concerned, the condition $\sigma_0 > 0$ denotes the existence of a significant density of cross-links that hinder macroscopic flows.

As shown in Fig. 5, Equation (1) perfectly fits the experimental η^* data, reassuring about the meaningfulness of the fitting parameters. The only exception is represented by the sample treated for 150 min in N_2, whose marked power law behavior impedes a reliable fitting using Equation (1). We stress once again that the curves obtained via simple frequency scans are noticeably distorted (see full circles in Fig. 5). This means that the following rheological analysis would not have been possible without resorting to TRMS.

Let us start the analysis of the fitting parameters of Equation (1). The time dependence of η_0^* is shown in Fig. 7. In entangled linear polymers, the zero-shear rate viscosity η_0, grows with the average molecular weight as $\eta_0 = kM_W^{3.4}$, k being a constant [28]. The previous relationship keeps working by referring to η_0^*, which in case

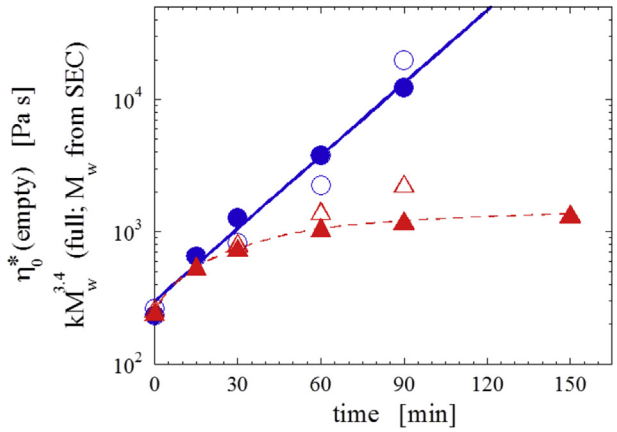

Fig. 7. Time evolutions of η_0^* (full symbols) for the samples treated in N_2 (blue circles) and in air (red triangles). The continuous thick line is the exponential fitting to the η_0^* data in N_2, while the thin dashed line is a guide for the eye. Empty symbols are the M_w data collected via GPC analyses, properly scaled to enable comparison with the η_0^* data ($k = 2.86 \times 10^{-3}$, M_w in kDa). (For interpretation of the references to colour in this figure legend, the reader is referred to the web version of this article.)

of pure polymers can be used in place of η_0 by invoking the Cox-Merz rule, $\eta(\dot{\gamma}) = \eta^*(\omega)$ for $\dot{\gamma} = \omega$ [32]. Therefore, in Fig. 7 we also show the M_w data from SEC properly scaled to enable direct comparison with η_0^*.

Consider first the sample treated in N_2. The values of η_0^* increase during time according to an exponential law. This indicates a second-order kinetics consistent with post-condensation of PA11, which is a first-order reaction in both amine and acid groups. The agreement between rheological and SEC data con-firms the direct relationship between η_0^* and M_w. Accordingly, MALDI-TOF analyses of the sample treated in N_2 reveal a pro-gressive disappearance of peaks assigned to COOH/NH_2 termi-nated oligomers (see Figure S4, Supplementary data). Such signals reappear over long times (120 min), likely due to concomitant hydrolysis reactions promoted by water produced during the former post-condensation.

Now consider the sample treated in air. The increase of η_0^* in the early stages of the test is comparable with the one observed in N_2. This is not surprising, since only the edge of the disk-shaped sample is actually exposed to air. As a result, the nature of the surrounding gas initially has a negligible effect, and the degradation kinetics reflects the same thermally-activated mechanisms as in N_2. As time goes on, oxygen and water molecules from the air environment diffuse inside the polymer and activate specific thermo-oxidative phenomena. At the macroscopic scale of rheological tests, the
overall effect is a slackening of the growth of η_0^*, which reaches a steady state value in about 60 min. This is ascribed to concurrent chain scission events, which balance the increase in M_w because of post-condensation. Accordingly, SEC data indicate a slowdown of the growth of M_w after 60 min; at the same time, signals of low-molecular weight compounds are detected by MALDI-TOF (not shown). Among others, NH_2/COOH oligomers derive from hydrolysis reactions promoted by air humidity, while low-molecular weight compounds having amide terminal groups are the result of thermo-oxidative degradation [19,20,23]. The latter species, directly involved in cross-linking reactions, gradually disappear; meanwhile, a fraction of insoluble gel forms. This aspect will be discussed in more detail in *Part II* [25]. Here we simply observe that the agreement discussed above between η_0^* data and SEC and MALDI analyses only concerns the fraction of polymer that actually dissolves in the solvent. The remaining insoluble gel, not directly analyzable through SEC and MALDI, plainly appears in the rheological tests as a yield stress σ_0. The latter parameter is shown in Fig. 8 as a function of time.

Negligible yield stresses are required to fit the η^* curves of the samples treated in N_2. This is confirmed by the absence of insoluble gel fractions in these samples. The same happens in air for times shorter than 60 min. Recently, Okamba-Diogo et al. proposed that cross-linking of PA11 only begins after an induction time, presumably because it involves reactions among primary oxidation products [33]. Once cross-linking has started the growth of σ_0 is fast, and the concomitant increase of insoluble gel corroborates the relationship between cross-linking reactions and the appearance in rheological curves of a yield stress.

Before concluding the rheological analysis by discussing the remaining two rheological parameters, it is important to emphasize the ability of rheological analysis of distinguish between uncross-linked and cross-linked polymer fractions coexisting in the sample treated in air. This is a consequence of the well distinct relaxation timescales of these two dynamic populations. Regarding the cross-linked fraction, it is useful to add a geometrical consideration. In parallel plate configuration cross-linking starts from the sample edge, where the polymer is in direct contact with air, and gradually proceeds towards the center while the gases diffuse inside the sample. Both the inner, still not cross-linked portion of sample, and the outer, cross-linked annulus of width δ, contribute to the mo-mentum Ω, from which the shear stress σ and all related rheological functions are derived (see Fig. 9). Nevertheless, being farther from the rotation axis, the outer shell contributes most to Ω. In other words, it is as if the rheological response of the cross-linked fraction was amplified, making it promptly detectable through rheological measurements in parallel plate geometry. Similar arguments should be taken into account when other flow geometries are used.

Finally, let us consider the remaining two fitting parameters of Equation (1), which are shown in Fig. 10 as a function of time.

Differently from σ_0, both λ and n uniquely refer to the uncross-linked fraction of polymer. The main relaxation time is directly correlated to the molecular weight. As such, λ essentially follows the same trend as η_0^*: it increases with time in N_2, while a plateau value is reached in air in about 60 min.

As far as the non-Newtonian feature of the polymer is concerned, a comparable decrease of the flow index n is noticed in both environments. The chain extension and/or scission phenomena occurring during rheological tests bring about a widening of the

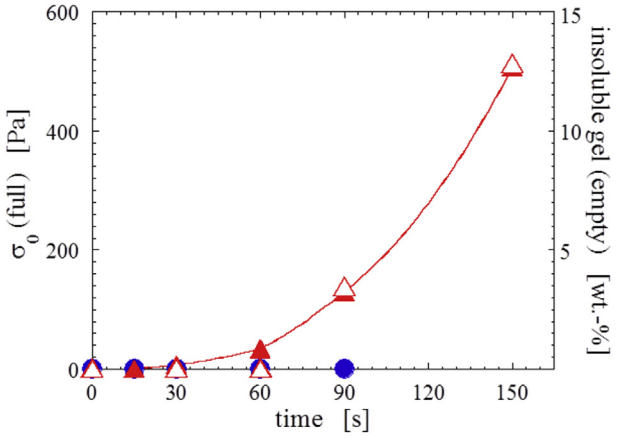

Fig. 8. Time evolutions of σ_0 (a) for the samples treated in N_2 (blue circles) and in air (red squares). The amount of insoluble gel in the air-treated samples is also reported on the right axis of (a) (red triangles; empty). Line is a guide-to-the eye. (For interpretation of the references to colour in this figure legend, the reader is referred to the web version of this article.)

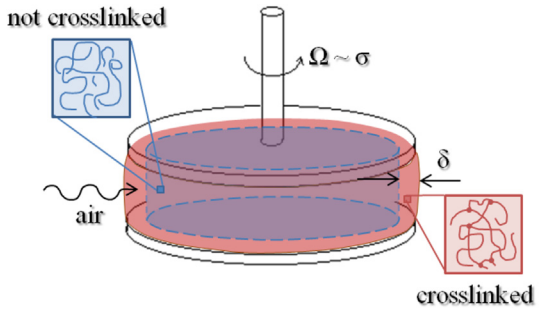

Fig. 9. Schematic of degradation for the sample subjected to rheological measurements in parallel plate geometry. After an induction time, cross-linking starts from the sample edge and proceeds towards the center.

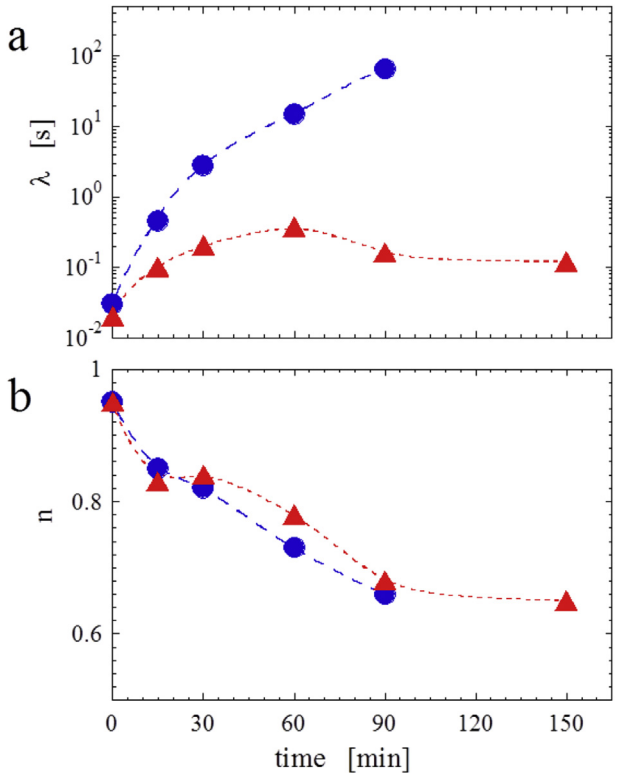

Fig. 10. Time evolutions of λ (a) and n (b) for the samples treated in N_2 (blue circles) and in air (red squares). Lines are guide-to-the eye. (For interpretation of the references to colour in this figure legend, the reader is referred to the web version of this article.)

MMDs. SEC-MALS analyses show that the consequent increase over time of the polydispersity index, M_w/M_n, is comparable for the two samples (see Table 1). As a result, a similar accentuation of the non-Netwtonian feature is noticed in the two cases.

Table 1
Molar masses as determined through SEC-MALS.

Sample	M_n [kDa]	M_w [kDa]	M_w/M_n
Virgin PA11	16.8	28.8	1.72
30 min in N2	20.9	40.4	1.94
60 min in N2	24.1	54.2	2.25
90 min in N2	41.9	102.8	2.45
30 min in air	20.5	40.3	1.96
60 min in air	21	47.4	2.25
90 min in air	25.2	57.6	2.28

Conclusions

Degradation of PA11 in the melt state in both oxidative and non-oxidative conditions has been studied with rheological and analytical techniques. In both environments the polymer experiences fast alterations in the molecular architecture, which prevents the collection of rigorous data via usual rheological analysis. Changes in the rheological properties while testing have been eluded by means of TRMS. Such an approach has enable us to infer the linear viscoelasticity of "virgin" PA11, i.e. before the occurrence of any degradation phenomenon. In addition, snapshots of the viscoelastic behavior have been collected in the course of degradation, and the data have been correlated to the advance of degradation phenomena. Clear differences have emerged between the samples treated in N_2 and in air. In particular, a gradual increase of the viscoelastic moduli takes place in the former case, without significant alterations of the overall relaxation spectrum. Differently, a clear arrest of relaxation dynamics occurs in air after about 60 min. Further information has been gathered by studying the time evolution of the complex viscosity. A Carreau-like equation with a yield stress has revealed to be adequate for fitting the experimental η^* data, providing, among others parameters, the zero−frequency complex viscosity and the yield stress. The former is correlated to the average molecular weight, while the latter reflects the existence of a significant density of cross-links that hinder macroscopic flows. The time evolutions of the rheological parameters have resulted in good agreement with SEC-MALS data. Moreover, a preliminary MALDI-TOF study has shed light on the chemical aspects of degradation. In particular, post-condensation is the dominant degradation mechanism of PA11 in inert N_2 atmosphere, whereas three distinct thermo-oxidative processes take place in air, namely post-condensation, chain scission and cross-linking. The latter require an induction time of about 60 min.

Although the need of targeted analytical techniques for a deep understanding of the degradation pathways is unquestionable, the present study demonstrates that rheology is a valuable tool for studying polymer degradation in the melt state, being able to detect and even discriminate among the different degradation mechanisms. In particular, rheology has proved to be very sensitive to cross-linking reactions. The latter can be difficult to be detected using techniques like SEC-MALS and MALDI-TOF, which require the solubilization of the sample. Pros and cons of rheological analyses are further discussed in *Part II* [25], in which nanoparticles are added to PA11 in order to alter the rheology of the sample, possibly screening the effects of polymer degradation.

Acknowledgments

This work was supported by the FIRB 2010−Futuro in ricerca project (No. RBFR10DCS7) funded by the Italian Ministry of University and Research (MIUR).

Appendix A. Supplementary data

Supplementary data related to this article can be found on line.

References

[1] M. Mours, H.H. Winter, Time-resolved rheometry, Rheol. Acta 33 (5) (1994) 385−397, http://dx.doi.org/10.1007/BF00366581.
[2] C.R. López-Barrón, C.W. Macosko, Rheology of compatibilized immiscible blends with droplet-matrix and cocontinuous morphologies during coarsening, J. Rheol. (1978-present) 58 (6) (2014) 1935−1953, http://dx.doi.org/10.1122/1.4897409.

[3] W. Liu, X. Dong, F. Zou, J. Yang, D. Wang, C.C. Han, Morphology evolution and rheological properties of polybutadiene/polyisoprene blend after the cessation of steady shear, J. Chem. Phys. 139 (11) (2013) 114904, http://dx.doi.org/10.1063/1.4821175.

[4] J.K. Yeganeh, F. Goharpey, R. Foudazi, Can only rheology be used to determine the phase separation mechanism in dynamically asymmetric polymer blends (PS/PVME)? RSC Adv. 2 (21) (2012) 8116–8127, http://dx.doi.org/10.1039/C2RA21307A.

[5] H.H. Winter, F. Chambon, Analysis of linear viscoelasticity of a crosslinking polymer at the gel point, J. Rheol. (1978-present) 30 (2) (1986) 367–382, http://dx.doi.org/10.1122/1.549853.

[6] M. Wang, H.H. Winter, G.K. Auernhammer, Time and frequency dependent rheology of reactive silica gels, J. Colloid Interface Sci. 413 (2014) 159–166, http://dx.doi.org/10.1016/j.jcis.2013.09.035.

[7] C.Y.M. Tung, P.J. Dynes, Relationship between viscoelastic properties and gelation in thermosetting systems, J. Appl. Polym. Sci. 27 (2) (1982) 569–574, http://dx.doi.org/10.1002/app.1982.070270220.

[8] L. Núñez-Regueira, C.A. Gracia-Fernández, S. Gómez-Barreiro, Use of rheology, dielectric analysis and differential scanning calorimetry for gel time determination of a thermoset, Polymer 46 (16) (2005) 5979–5985, http://dx.doi.org/10.1016/j.polymer.2005.05.060.

[9] R.J. Sheridan, C.N. Bowman, A simple relationship relating linear viscoelastic properties and chemical structure in a model Diels–Alder polymer network, Macromolecules 45 (18) (2012) 7634–7641, http://dx.doi.org/10.1021/ma301329u.

[10] X. Wang, P. Sun, G. Xue, H.H. Winter, Late-state ripening dynamics of a polymer/clay nanocomposite, Macromolecules 43 (4) (2010) 1901–1906, http://dx.doi.org/10.1021/ma901665m.

[11] J.S. Wheeler, S.W. Reynolds, S. Lancaster, V.S. Romanguera, S.G. Yeates, Polymer degradation during continuous ink-jet printing, Polym. Degrad. Stab. 105 (2014) 116–121.

[12] F. Carrasco, P. Pagès, J. Gámez-Pérez, O.O. Santana, M.L. Maspoch, Processing of poly (lactic acid): characterization of chemical structure, thermal stability and mechanical properties, Polym. Degrad. Stab. 95 (2) (2010) 116–125, http://dx.doi.org/10.1016/j.polymdegradstab.2009.11.045.

[13] F.P. La Mantia, V. Città, A. Valenza, S. Roccasalvo, Influence of low extents of degradation on the processing behaviour of high density polyethylene, Polym. Degrad. Stab. 23 (2) (1989) 109–119, http://dx.doi.org/10.1016/0141-3910(89)90082-7.

[14] V. Mailhos-Lefievre, D. Sallet, B. Martel, Thermal degradation of pure and flame-retarded polyamides 11 and 12, Polym. Degrad. Stab. 23 (4) (1989) 327–336, http://dx.doi.org/10.1016/0141-3910(89)90055-4.

[15] W. Romão, E.V. Castro, A.S. Elói Filho, R.C. Guimarães, A.L. Silva, S. Teixeira, G.L. De Sena, Ageing of polyamide 11 used in the manufacture of flexible piping, J. Appl. Polym. Sci. 114 (3) (2009) 1777–1783, http://dx.doi.org/10.1002/app.30793.

[16] E. Richaud, O.O. Diogo, B. Fayolle, J. Verdu, J. Guilment, F. Fernagut, Review: auto-oxidation of aliphatic polyamides, Polym. Degrad. Stab. 98 (9) (2013) 1929–1939, http://dx.doi.org/10.1016/j.polymdegradstab.2013.04.012.

[17] S.V. Levchik, L. Costa, G. Camino, Effect of the fire-retardant, ammonium polyphosphate, on the thermal decomposition of aliphatic polyamides. I. Polyamides 11 and 12, Polym. Degrad. Stab. 36 (1) (1992) 31–41, http://dx.doi.org/10.1016/0141-3910(92)90045-7.

[18] B.J. Holland, J.N. Hay, Thermal degradation of nylon polymers, Polym. Int. 49 (9) (2000) 943–948, 10.1002/1097-0126(200009)49:9<943::AID-PI400>3.0.CO;2–5.

[19] D. Chionna, C. Puglisi, F. Samperi, G. Montaudo, A. Turturro, Thermal oxidation products of nylon 6 determined by MALDI-TOF mass spectrometry, Macromol. Rapid Commun. 22 (7) (2001) 524–529, 10.1002/1521-3927(20010401)22:7<524::AID-MARC524>3.0.CO;2-B.

[20] S. Carroccio, C. Puglisi, G. Scaltro, T. Ferreri, G. Montaudo, Matrix-assisted laser desorption/ionization time-of-flight investigation of Nylon 6 and Nylon 66 thermo-oxidation products, Eur. J. Mass Spectrom. 13 (6) (2008) 397–408, http://dx.doi.org/10.1255/ejms.899.

[21] M. Lozano-González, M. Rodriguez-Hernandez, J. Villalpando-Olmos, Physical–mechanical properties and morphological study on nylon-6 recycling by injection molding, J. Appl. Polym. Sci. 76 (6) (2000) 851–858, 10.1002/(SICI)1097-4628(20000509)76:6<851::AID-APP11>3.0.CO;2-D.

[22] S. Acierno, P. Van Puyvelde, Rheological behavior of polyamide 11 with varying initial moisture content, J. Appl. Polym. Sci. 97 (2) (2005) 666–670, http://dx.doi.org/10.1002/app.21810.

[23] M.J. Oliveira, G. Botelho, Degradation of polyamide 11 in rotational moulding, Polym. Degrad. Stab. 93 (1) (2008) 139–146, http://dx.doi.org/10.1016/j.polymdegradstab.2007.10.004.

[24] M.J. Oliveira, M.C. Cramez, C.B. Garcia, M.P. Kearns, E. Maziers, Effect of the processing conditions on the microstructure and properties of rotational molded polyamide 11, J. Appl. Polym. Sci. 108 (2) (2008) 939–946, http://dx.doi.org/10.1002/app.27344.

[25] G. Filippone, S.C. Carroccio, G. Curcuruto, E. Passaglia, C. Gambarotti, N.Tz. Dintcheva, Time-resolved rheology for studying polymer degradation in the melt – part II: Thermal and Thermo-oxidative Degradation of Polyamide 11/organo-clay Nanocomposites. (Submitted to Polymer).

[26] R. Mendichi, A.G. Schieroni, Current trends in polymer science, in: Use of a Multi-detector Size Exclusion Chromatography System for the Characterization of Complex Polymers. Trivandrum, India: Pandalai, 6, 2001, pp. 17–32.

[27] P.J. Wyatt, Light scattering and the absolute characterization of macromolecules, Anal. Chim. Acta 272 (1) (1993) 1–40.

[28] J.D. Ferry, Viscoelastic Properties of Polymers, John Wiley & Sons, 1980.

[29] The isochronal moduli were estimated as the intercepts between vertical lines and the interpolating curves, i.e. the segments connecting the experimental data. Specific software better suited to interpolate rheological data could have been used for this purpose, but the quite regular trend of our experimental data makes sufficiently accurate our graphical estimates.

[30] C. El-Mazry, M.B. Hassine, O. Correc, X. Colin, Thermal oxidation kinetics of additive free polyamide 6-6, Polym. Degrad. Stab. 98 (1) (2013) 22–36, http://dx.doi.org/10.1016/j.polymdegradstab.2012.11.002.

[31] P. Maréchal, R. Legras, J.M. Dekoninck, Post condensation and oxidation processes in molten polyamide 6, J. Polym. Sci. Part A: Polym. Chem. 31 (8) (1993) 2057–2067, http://dx.doi.org/10.1002/pola.1993.080310812.

[32] W.P. Cox, E.H. Merz, Correlation of dynamic and steady flow viscosities, J. Polym. Sci. 28 (1958) 619–622, http://dx.doi.org/10.1002/pol.1958.1202811812.

[33] O. Okamba-Diogo, E. Richaud, J. Verdu, F. Fernagut, J. Guilment, B. Fayolle, Molecular and macromolecular structure changes in polyamide 11 during thermal oxidation, Polym. Degrad. Stab. 108 (2014) 123–132, http://dx.doi.org/10.1016/j.polymdegradstab.2014.05.028.